The EMBO Journal (2004) 23, 2216–2225 | © 2004 European Molecular Biology Organization | All Rights Reserved 0261-4189/04
www.embojournal.org

THE EMBO JOURNAL

Talin B is required for force transmission in morphogenesis of *Dictyostelium*

Masatsune Tsujioka[1], Kunito Yoshida[2] and Kei Inouye*

Department of Botany, Graduate School of Science, Kyoto University, Sakyo-ku, Kyoto, Japan

Talin plays a key role in the assembly and stabilisation of focal adhesions, but whether it is directly involved in force transmission during morphogenesis remains to be elucidated. We show that the traction force of *Dictyostelium* cells mutant for one of its two talin genes *talB* is considerably smaller than that of wild-type cells, both in isolation and within tissues undergoing morphogenetic movement. The motility of mutant cells in tightly packed tissues *in vivo* or under strong resistance conditions *in vitro* was lower than that of wild-type cells, but their motility under low external force conditions was not impaired, indicating inefficient transmission of force in mutant cells. Antibody staining revealed that the *talB* gene product (talin B) exists as small units subjacent to the cell membrane at adhesion sites without forming large focal adhesion-like assemblies. The total amount of talin B on the cell membrane was larger in prestalk cells, which exert larger force than prespore cells during morphogenesis. We conclude that talin B is involved in force transmission between the cytoskeleton and cell exterior.

The EMBO Journal (2004) **23,** 2216–2225. doi:10.1038/sj.emboj.7600238; Published online 13 May 2004
Subject Categories: cell & tissue architecture
Keywords: cytoskeleton; *Dictyostelium*; morphogenesis; talin; traction force

Introduction

Force is an important component of morphogenesis. In developmental processes involving cell migration and tissue shape changes, the force generated by molecular motors within the cells has to be effectively transmitted to the extracellular matrix from which they get traction. Molecules involved in the interaction between the extracellular matrix, cell membrane and cytoskeleton are therefore important in understanding the mechanism of morphogenesis.

Talin is a large cytoskeletal protein (Burridge and Connell, 1983) with a molecular mass of ca. 270 kDa containing integrin-, F-actin- and vinculin-binding domains (reviewed in Critchley, 2000). In metazoan cells, this protein is localised in cell adhesion structures such as focal contacts (Burridge and Connell, 1983) and myotendinous junctions (Tidball *et al*, 1986). Since these structures are subject to large tensile forces, it was suggested that talin may be a force-transmitting molecule. Later studies using antibody microinjection (Nuckolls *et al*, 1992; Bolton *et al*, 1997), antisense inhibition (Albigès-Rizo *et al*, 1995) and gene disruption (Priddle *et al*, 1998) have revealed a role of talin in the assembly and stabilisation of focal adhesions, while the question as to whether talin is directly involved in force transmission across the cell membrane is yet to be answered.

Apart from the role of talin in attachment of cells to the substratum, its role in development remained unknown until recently. The first evidence for the involvement of talin in development came from a study of a talin homologue in *Dictyostelium* (Tsujioka *et al*, 1999), which will be described in some detail below. In the mouse, knockout of one of the talin genes was shown to result in incomplete gastrulation leading to embryonic death (Monkley *et al*, 2000). Homozygous mutants of the single talin gene in *Drosophila* show a failure in germ band retraction and pronounced muscle detachment (Brown *et al*, 2002). These results indicate important roles of talin during morphogenesis.

The purpose of the present study is to examine whether talin mediates transmission of force during multicellular morphogenesis in *Dictyostelium*. This eukaryotic microorganism displays a remarkable series of morphogenetic movements of multicellular structures composed of highly motile cells, and it shares much of its basic machinery of multicellular morphogenesis with metazoan development (Coates and Harwood, 2001). One of the advantages of using this organism in studies of morphogenesis is its structural simplicity; force generated by a tissue undergoing morphogenesis can be measured and simple interpretation of the results is possible. The first multicellular structure formed is a hemispherical structure called the 'mound'. A small protrusion called the tip emerges from the top of the mound, which then elongates to form a cylindrical structure known as a 'slug'. Prestalk and prespore cells differentiate within mounds, where the majority of prestalk cells accumulate to the apical regions and lead morphogenetic movements of the slug throughout multicellular development (Raper, 1940; Rubin and Robertson, 1975).

Two genes (*talA* and *talB*) that encode talin homologues have been identified in *Dictyostelium* (Kreitmeier *et al*, 1995; Tsujioka *et al*, 1999). Interestingly, their products talin A (encoded by *talA*) and talin B (encoded by *talB*) have distinct functions in this organism. While talin A has a function during growth and the single-cell phase of development (Niewöhner *et al*, 1997; Simson *et al*, 1998; Merkel *et al*, 2000), morphogenesis after the mound stage is unaffected by disruption of *talA*. By contrast, *talB* mutant cells grow and develop normally up until they form tight mounds, but the development is completely blocked at that stage.

*Corresponding author. Department of Botany, Graduate School of Science, Kyoto University, Sakyo-ku, Kyoto 606-8502, Japan.
Tel.: +81 75 753 4130; Fax: +81 75 753 4137;
E-mail: inoue@cosmos.bot.kyoto-u.ac.jp
[1]Present address: Wellcome Trust Biocentre, School of Life Science, University of Dundee, Dow Street, Dundee DD1 5EH, UK
[2]Present address: Department of Biological Sciences, Sir Alexander Fleming Building, Imperial College London, London SW7 2AZ, UK

Received: 20 January 2003; accepted: 21 April 2004; published online: 13 May 2004

Examination using prestalk and prespore differentiation markers showed that mutant cells differentiate normally within the mounds and, when mixed with a sufficient number of wild-type cells, they participate in the morphogenetic movement and differentiate into stalk cells and spores upon fruiting body formation (Tsujioka *et al*, 1999).

In this study, using the wild-type and *talB* mutant strains, we measured the force generated by slugs during migration and also examined the motility and traction force of isolated cells under different magnitudes of resistance. We further investigated subcellular as well as tissue-level localisation of talin B in detail using an antibody directed to a partial sequence of the protein. The results obtained provide evidence for the involvement of talin B in force transmission at the membrane–cytosol interface.

Results

Mutant strains

Mutant strains with a disrupted *talB* gene (HKT102, HKT104 and HM1011) were obtained by gene replacement by homologous recombination with plasmids carrying different disruption constructs (Figure 1A; Tsujioka *et al*, 1999). The phenotype of HKT102 and HM1011 has been described previously (Tsujioka *et al*, 1999), and that of the newly isolated mutant HKT104 was essentially identical to those of the other *talB* mutants.

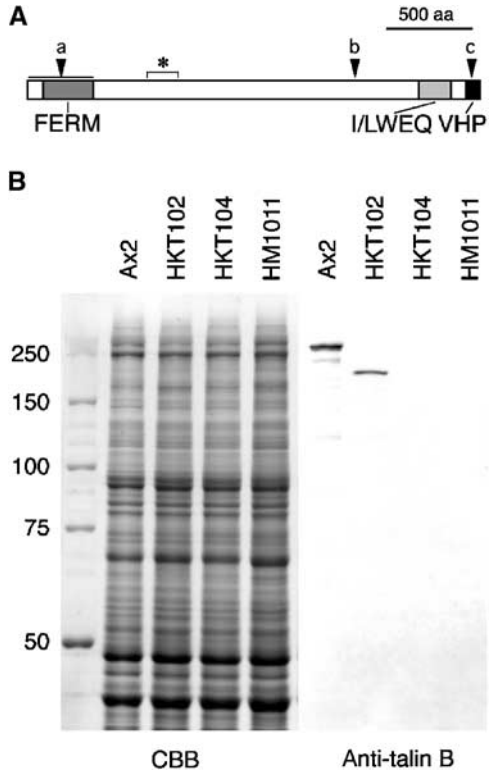

Figure 1 (**A**) Schematic representation of talin B. The FERM domain, I/LWEQ domain and villin headpiece homology domain (VHP) are shown. Asterisk indicates the antigen region for the antibody, and arrowheads the positions of insertion or replacement of the knockout constructs (a: HKT104; b: HKT102; c: HM1011). (**B**) Immunoblot demonstration of the polypeptides recognised by the anti-talin B antibody. Total cell lysates of the indicated strains were separated by SDS–PAGE, transferred to nitrocellulose filter and reacted with the antiserum (2000-fold dilution, right panel). Half the gel with duplicate lanes was stained with Coomassie blue (left panel).

A polyclonal antibody was raised against a bacterially expressed polypeptide corresponding to the region between the 737th and 876th amino-acid residues of talin B, which is downstream of the FERM domain and shows only low homology to talin A (amino-acid sequence identity 23%). Western blots of total cell extracts with this antibody (Figure 1B) indicated the presence of a polypeptide with an apparent molecular mass of 250 kDa in Ax2 and one of 190 kDa in HKT102, but there were no detectable bands in the extracts of HKT104 and HM1011. The nucleotide sequence of the inserted plasmid and the patterns of partial degradation products of the protein on Western blots (not shown) suggested that the 190 kDa polypeptide corresponds to a partial sequence of talin B from its N-terminal end to Ala1899 followed by nine amino-acid residues derived from the plasmid sequence. The presence of the truncated protein, albeit at a lower level, in HK102 suggests that the C-terminal region of the protein may be indispensable for its function during morphogenesis. This C-terminal region contains an I/LWEQ domain (McCann and Craig, 1997) and a villin headpiece-like domain, both implicated in interaction with F-actin (Figure 1A).

Measurement of force generated by migrating slugs

Motive force of a migrating slug can be determined by measuring the force that is just large enough to stall its advancement (balance force hereafter). In this study, we used hydrostatic pressure as the external force. To apply hydrostatic pressure along the length of a slug, each migrating slug was introduced into a capillary made in a hard agar block with a bore that fitted the slug. In reality, the force generated by a migrating slug is usually too large to be balanced by external force without causing excessive distortion of the agar. Therefore, the balance force was determined by measuring the velocity of slugs under various pressures (both positive and negative, here positive being counter-pressure) and extrapolating the linear regression line of the pressure–velocity relationship to the zero-velocity point for each slug (Inouye and Takeuchi, 1980). Since *talB* mutant cells do not form migrating slugs on their own, mutant and wild-type cells were mixed at a ratio of 1:1 and allowed to develop into chimeric slugs.

Figure 2A shows examples of the pressure–velocity relationship for chimeric slugs and a wild-type control of about the same size. It can be seen that the speed decreases linearly with increasing pressure in all slugs. The balance force was obtained by multiplying the pressure corresponding to the zero velocity with the cross-section of the slug. It has been shown that the balance force of a slug is approximately proportional to its volume, and therefore the force divided by the volume is a measure of the force exerted by a unit volume of cell averaged over the entire slug. Figure 2B summarises the results of all measurements. The motive forces of the chimeric slugs (16.2 and 14.6 $N\,cm^{-3}$ for HKT102 and HKT104, respectively) are clearly smaller than wild type (30.7 $N\,cm^{-3}$), with the difference being statistically significant.

It should also be noted in Figure 2A that at negative pressure (i.e. when the slug is pulled forward by the external

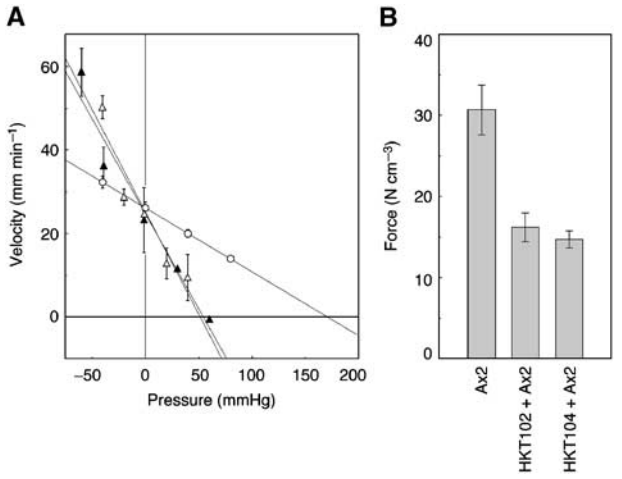

Figure 2 (**A**) Measurement of motive force of migrating slugs. Shown are examples of pressure–velocity relationship of an Ax2 slug (open circles) and chimeric slugs composed of Ax2 cells and *talB* mutant cells mixed at a 1:1 ratio (open triangles, HKT102; filled triangles, HKT104). Migrating velocity of each slug in an agar capillary is plotted against the hydrostatic pressure (relative to atmospheric pressure) applied to the anterior end of the slug. The posterior end of the slug was exposed to atmospheric pressure. Linear regression lines are drawn by the least square method. (**B**) Motive forces (in N cm^{-3}, mean ± s.e.m.) of Ax2 slugs and chimeric slugs were 30.7 ± 3.1 ($n = 13$), 16.2 ± 1.8 ($n = 9$) and 14.6 ± 1.1 ($n = 10$), respectively, the difference between Ax2 and the chimaeras being statistically significant ($P < 0.01$ by the Mann–Whitney test).

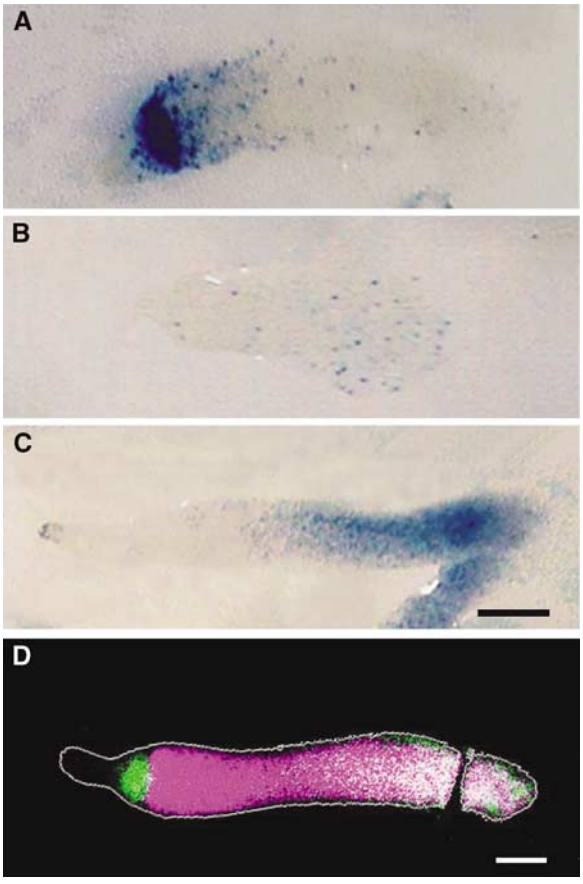

Figure 3 Cell-type marker expression in *talB* mutant cells in chimeric slugs. HKT102 cells expressing either *ecmAO-lacZ* (**A**), *ecmB-lacZ* (**B**) or *cotC-lacZ* (**C**) were mixed with Ax2 cells without marker at a ratio of 7:3 (A, B) or 9:1 (C), allowed to form slugs and subjected to *lacZ* staining. (**D**) Pseudocolour representation of a fluorescence micrograph of a chimeric slug composed of HKT104 cells labelled with fluorescein-dextran and unlabelled Ax2 cells stained with a rhodamine-conjugated antibody recognising prespore vacuoles (PSV). The contour of the slug is depicted in grey. Mutant cells are shown in green and prespore cells in magenta, and consequently wild-type prestalk cells appear black, mutant prestalk cells green, wild-type prespore cells magenta and mutant prespore cells white (due to the overlap of green and magenta). Scale bar: 100 μm.

pressure) the chimeric slugs, despite their smaller forces, moved even faster than the wild type. Considering that the speed of movement is determined by the balance between the propelling force and counteracting resistance, this reversal of speed in the negative pressure zone should mean that the total resistance to the movement is also small in the chimeric slugs.

Sorting patterns of prestalk and prespore cells in chimeric slugs

It has been shown that cells with larger motive force take up more anterior positions along the slug length, and this is proposed to be the primary cause of the antero-posterior pattern of prestalk and prespore cells in the slug (Inouye and Takeuchi, 1979; Umeda and Inouye, 2004). In chimeric slugs consisting of wild-type and *talB* mutant cells, the latter cells are often observed to form two bands, one at the 'neck' of the slug and the other at its 'tail' (Tsujioka *et al*, 1999). To identify the cell types in the 'neck' and 'tail' bands, mutant cells were transformed with a prestalk-specific *ecmAO-lacZ* construct (expressed in all prestalk cells), *ecmB-lacZ* construct (expressed in a subclass of prestalk cells some of which cluster near the tip of the slug and the rest scattering in the posterior zone), and a prespore-specific *cotC-lacZ* construct (Williams *et al*, 1989; Haberstroh and Firtel, 1990). Cells of each transformant were separately mixed with Ax2 cells at ratios of 1:9 to 3:7 (mutant:wild-type), allowed to form migrating slugs, and examined for β-galactosidase expression.

Figure 3 shows typical staining patterns obtained. In the chimaera composed of wild-type cells and *ecmAO-lacZ*-transformed *talB* mutant cells, *lacZ* staining (i.e. mutant prestalk cells) was invariably observed within the prestalk zone of the slug corresponding to the 'neck' band (Figure 3A). The few blue-stained cells in the prespore zone are anterior-like cells, a subpopulation of prestalk cells found in the prespore zone during slug migration (Sternfeld and David, 1981). In mixed slugs containing *talB* mutant cells with the *ecmB-lacZ* label, *lacZ*-positive cells of the mutant were observed only in the rear part of the slug (Figure 3B). In mixes of wild-type cells and *talB* mutant cells carrying the *cotC-lacZ* construct, almost all mutant cells expressing the *cotC-lacZ* construct were localised in the posterior half of the prespore region (Figure 3C). These results demonstrate that prestalk and prespore cells of the *talB* mutant strain were sorted out behind their wild-type counterparts within the chimeric slugs. This conclusion was confirmed in double-staining experiments using cell-type-specific antibody with chimaeras consisting of fluorescently labelled mutant cells and unlabelled wild-type cells (Figure 3D). These results suggest that mutant cells are inefficient in exerting force within multicellular tissues.

If the mutant:wild-type ratio of the chimaera was too high (4:6 to 6:4), slugs often split transversely to leave their posterior parts behind as a large lump of cell mass consisting predominantly of mutant cells. If the percentage of mutant cells was even higher (7:3 to 9:1), the cells remained as mounds without forming a tip.

Motility and traction force of dissociated cells

To test whether the difference in the force exists in cells in isolation, wild-type and *talB* mutant cells were allowed to develop separately up to the mound stage, dissociated into single cells, and subjected to cell motility assay and traction force measurement. Normally, dissociated cells of *Dictyostelium* in buffer solution do not sufficiently adhere to the substratum and are unable to locomote effectively even though they actively extend pseudopodia; however, if confined in a thin layer of liquid, they show active movement in a manner very similar to that within migrating slugs (Yoshida and Inouye, 2001; Inouye, 2003). In the cell motility assay, dissociated cells were placed between two layers of agar, where the magnitude of mechanical resistance to cell movement was controlled by changing the space between the agar sheets.

Under conditions where the cells can move freely without strong mechanical resistance, both wild-type and mutant cells showed active locomotion, and the motility of mutant cells was comparable to wild type. Under strong mechanical resistance, by contrast, only a small fraction of the *talB* mutant cells moved over a significant distance and their mean velocity was very small, while wild-type cells still showed active locomotion (Table I). The defective motility of *talB* mutant cells dissociated from mounds was first noted by Cole (1997) with another *talB* mutant strain derived from the DH1 background.

The above results indicate that *talB* mutant cells are defective in exerting force on the substratum. To test this possibility, we attempted to measure the traction force of dissociated mound cells using elastic polyacrylamide substrata containing fluorescent beads as position markers. As in the previous assay, dissociated cells were placed between two layers of elastic substrata, and their movements as well as the positions of marker beads were recorded with a confocal microscope. Cellular forces were assumed to be exerted on the substratum by discrete small patches uniformly distributed over the cell surface, and their magnitude and direction were deduced from the marker displacement data by solving the equations of linear elasticity theory followed by statistical evaluation (Schwarz *et al*, 2002).

Figure 4B shows a typical force pattern of a locomoting wild-type cell. Here, the density of the force-transmitting points was set to be about 1/4 the mean density of the talin B-rich dots described below (cf. Figure 6). In many cells, the force field was not uniform, showing a few areas of relatively large forces, which were mostly stationary with respect to the substratum, as the cell advanced. Soft substrata were

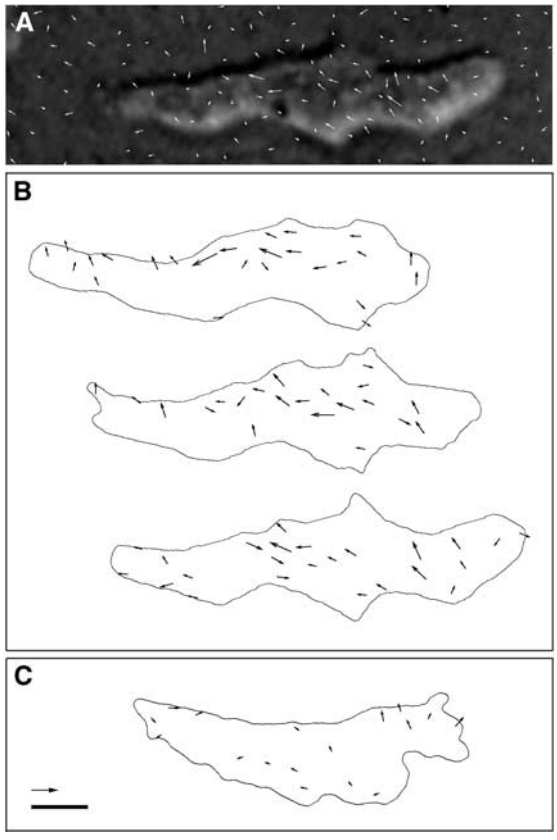

Figure 4 Force vector fields of a locomoting Ax2 cell. (**A**) Example of marker displacements overlaid on the photograph of the cell. The vectors are shown twice the actual size. (**B**) Deduced force vectors shown at 10 s intervals from top to bottom on the same horizontal coordinate. The forces were calculated from the marker displacement data at each time point (the one shown in (A) corresponds to the last figure of (B)) at grid points of 1.6 μm intervals. (**C**) Deduced force vectors of an HKT104 cell. Values not exceeding the noise level are not shown. Scale bar: 5 μm; arrow: 200 pN.

Table I Movement of wild-type and *talB* mutant cells in response to cAMP gradient

Strain	% cells moving towards cAMP source			Locomotion speed (μm min^{-1})		
	Strong resistance	Weak resistance	Ratio	Strong resistance	Weak resistance	Ratio
Ax2	49.9±7.5 (10)	55.7±7.4 (9)	0.90	3.09±0.31 (100)	6.05±0.85 (66)	0.51
HKT102	8.4±3.8 (11)*	54.4±7.8 (6)	0.16	1.09±0.27 (59)**	5.68±0.47 (51)	0.19
HKT104	4.1±0.3 (11)*	50.5±5.7 (8)	0.08	1.39±0.20 (56)**	7.12±0.65 (84)	0.19

Dissociated cells at the mound stage were plated between agar sheets with two conditions of mechanical resistance, and a fine glass capillary containing cAMP solution was inserted as a chemoattractant source. In the left half of the table, percentage of the cells that moved towards the cAMP source within 15 min (see Materials and methods for details of the criteria) are shown as means±s.e.m. (number of experiments). In the right half, mean translocation speeds of the cells are shown (number of cells in parentheses). Ratios of the values under strong resistance to those under weak resistance are also shown. The differences between wild-type and each of the mutant strains in the values under the strong resistance condition are statistically significant (*$P<0.01$, **$P<0.001$).

required for mutant cells to migrate, and the deduced forces were significantly lower than wild-type cells moving on the same substrata (Figure 4C). The magnitude of the forces per unit area averaged ca. 129 ± 20 Pa ($n = 8$) for wild-type cells and 62 ± 6 Pa ($n = 7$) for mutant cells. These results are consistent with the cellular force estimated from the *in situ* measurements shown above, and provide further support for the defects of *talB* mutant cells in force transmission.

Localisation of talin B

If the function of talin B is force transmission between the cytoskeleton and cell adhesion molecules, the presence of larger numbers of talin B molecules subjacent to the cell membrane would be required in prestalk cells than in prespore cells. To confirm this, subcellular and tissue level localisation of talin B was investigated using the antibody directed to part of the talin B polypeptide shown in Figure 1.

In undifferentiated cells, talin B was predominantly distributed in regions near the cell membrane closely apposed to the substratum and at sites of cell-to-cell adhesion (Figure 5A). Simultaneous staining with fluorescent phalloidin indicates an overall tendency of colocalisation of talin B and F-actin, but unlike the latter the former showed speckled patterns of staining (Figure 5B). At the multicellular stage, pronounced accumulation of talin B to the cell membrane was evident in both prestalk and prespore cells, while weak yet significant staining persisted in the cytosol, often accumulating in the front of the cell (Figure 5C–E). Double staining with an antibody that recognises prespore vacuoles (PSVs) indicates that prestalk cells are more strongly stained with the talin B antibody (see below). Speckled staining patterns were often observed when focused on the cell membrane. This staining pattern was particularly conspicuous when tissues were flattened between a coverslip and agar. Under such conditions, cells move out from the tissue, forming streams of cells flowing outwards without losing their prestalk/prespore differentiation characters. When focused on the cell membrane of such cells directly attached to the external substratum, numerous small dots of fluorescence were invariably seen (Figure 5F). On focal planes cutting through the cells, strong staining was concentrated on the cell border as a row of fluorescent dots (Figure 5G). Fluorescent dots on the membrane with high staining intensity were more abundant, and the average intensity per area significantly higher, in prestalk cells than in prespore cells (Figure 6).

During fruiting body formation, the prestalk-enriched distribution of talin B became even more pronounced, and the difference in the intensity of talin B antibody staining at the prestalk–prespore boundary was very clear without exception in over 100 culminating slugs examined (Figure 7). In particular, regions of cell membranes near, but not directly apposed to, the stalk tube were heavily stained with the antibody. These regions are very close to the sites of adherens junctions where actin filaments and the *Dictyostelium* β-catenin homologue Aardvark are shown to be concentrated (Grimson *et al*, 2000). Densitometry measurements along the cell borders indicate that the peak of talin B distribution was ca. 1200 nm distal from the surface of the stalk in average, which can be distinguished from the radial distributions of F-actin and myosin II, both peaking at ca. 600–800 nm from the stalk surface (Figure 7B and E; see also Figure 1 of Grimson *et al*, 2000).

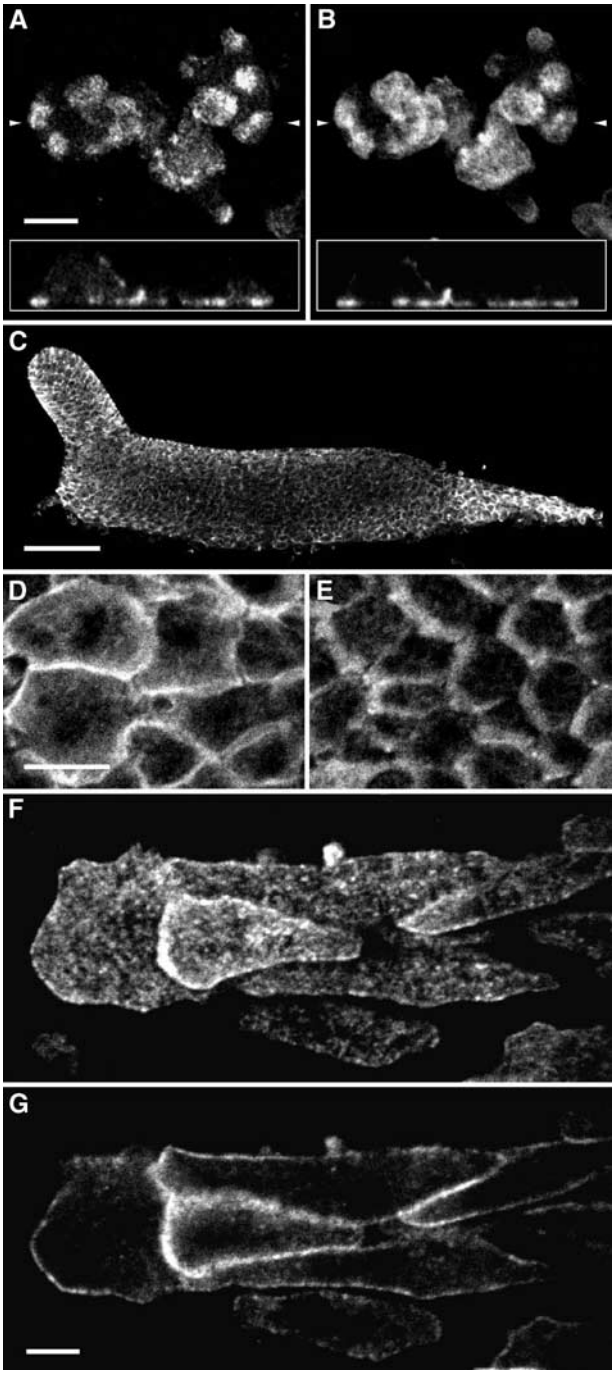

Figure 5 Localisation of talin B in cells at unicellular and multicellular stages of Ax2. (**A, B**) Cells at the growth phase were fixed with ethanol–formaldehyde and double-stained with the anti-talin B antibody (A) and fluorescent phalloidin (B). Focal plane immediately above the glass surface is shown. Insets show vertical sections reconstructed from horizontal sections made at intervals of 178 nm. Scale bar: 5 μm. The positions of the vertical sections are indicated by small arrows. (**C**) Whole-mount staining of a migrating slug with anti-talin B antibody. Anterior to the left. Scale bar: 50 μm. (**D, E**) Cells in the anterior prestalk region (D) and in the prespore region (E) at a higher magnification. Direction of cell movement is to the left. Scale bar: 10 μm. (**F, G**) Cells migrating away from a flattened slug. Focal planes right above the glass surface (F) and 500 nm above (G) are shown. Scale bar: 5 μm.

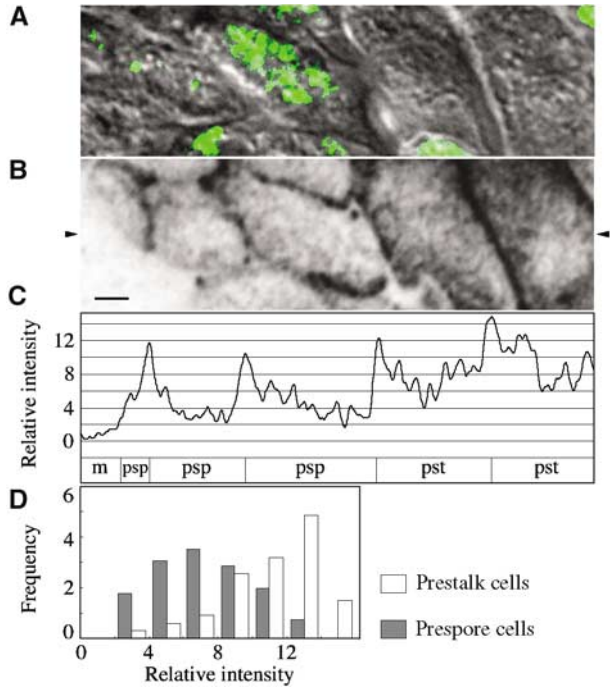

Figure 6 Fluorescent intensity distribution of fluorescent spots observed on the cell membrane of prestalk and prespore cells. A small area of a single slug sample is shown as an example of densitometry measurements. Cells of a flattened slug composed of wild-type and *talB* null (HM1011) cells (added as internal control) were double-stained with antibodies against PSV and talin B. (**A**) Nomarski image (greyscale) and PSV staining (green). Focal plane 2.15 μm above that of the image in (B) is presented to show PSVs. (**B**) Talin B staining. Focal plane right above the glass surface is shown. The original fluorescence image has been inverted for densitometry and then smoothed to eliminate noise components with wavelengths shorter than the theoretical spatial resolution of the optical system. Scale bar: 2 μm. (**C**) Density profile along the horizontal line indicated with the arrowheads in (B) to show the spatial resolution of fluorescent spots. The cell type along this line is shown below the density profile (pst: prestalk; psp: prespore; m: *talB* mutant prestalk). Ordinate indicates relative staining intensity with zero at the background staining determined from mean grey-scale values of 12 null mutant cells present in the visual field (of which one is seen in (A, B)). The unit is the root mean square of the noise of the image (defined as the difference between the original and smoothed image). (**D**) Histograms of the peak staining intensity of fluorescent spots in wild-type prestalk cells (open bars) and prespore cells (closed bars). Abscissa indicates relative intensity as expressed in the same unit as in (C), and ordinate the frequency in 0.1 dot μm^{-2}. Fluorescent spots with peak intensity over 2 units were scored in a total of 42 wild-type cells present in a single visual field that could be identified as either prestalk cells ($n = 11$) or prespore cells ($n = 31$). The intensity of staining relative to the overall average for the 42 cells was 1.52 ± 0.07 (mean $\pm$ s.e.m.) for prestalk cells and 0.81 ± 0.04 for prespore cells. Nonspecific staining defined by the staining of null mutant cells (0.29 ± 0.03, $n = 10$) has been subtracted from these values. The mean density of the fluorescent spots was 1.4 μm^{-2} for both cell types. Cell border regions where individual spots could not be distinguished were excluded from the measurements.

Discussion

Talin has been proposed to be a major link between the actin cytoskeleton and cell adhesion proteins that bind to the extracellular matrix. However, evidence for its involvement in force transmission during morphogenesis has been lacking. In the present study, we have demonstrated that talin B is indeed required for efficient exertion of force by *Dictyostelium* cells participating in multicellular morphogenesis. Although indirect effects cannot be ruled out, we would propose that a major function of talin B would be to link mechanically the actin cytoskeleton to the substratum outside via an integrin-type membrane protein. The close association of talin B with the cell membrane along with actin filaments, as well as its enrichment in prestalk cells, which generate large force during morphogenesis, is consistent with its proposed function.

Why is talin B required for tip formation?

The requirement of talin B for efficient exertion of force upon the substratum would explain the failure of *talB* mutant cells to form the tip. In a mound, a tip is formed at the site where prestalk cells have accumulated (Early *et al*, 1995). Formation of a tip probably requires large force since it involves drastic changes in the curvature of the tissue surface, which is covered with the cellulose-containing extracellular matrix (Freeze and Loomis, 1977). This view is supported by the inability of tip formation in some mutants that have defects in components of the cytoskeleton. For example, mutants lacking the heavy chain of myosin II do not show the sorting of prestalk cells to the apex of the mound and cannot form the tip (Springer *et al*, 1994; Traynor *et al*, 1994). Likewise, the absence of myosin regulatory light chain results in abnormal distribution of myosin heavy chain within the cell and the failure of tip formation (Chen *et al*, 1994). Mutants lacking both α-actinin and gelation factor (ABP120) are severely defective in tip formation (Witke *et al*, 1992). In *talB* mutants, even though prestalk cells sort to the position where a tip would normally form, no clear tip has ever been observed (Tsujioka *et al*, 1999). Therefore, the inability of *talB* mutants to form the tip is most likely a consequence of the reduced force of the mutant prestalk cells.

Sorting-out of talB mutant cells in chimeric slugs

The sorting pattern of *talB* mutant cells in chimeric slugs can be interpreted as a consequence of the balance of the three forces acting on each cell within the slug: (1) the motive force of the cell, (2) internal resistance to its movement, and (3) the external force acting on it (Inouye and Takeuchi, 1979; Umeda and Inouye, 2004). Since there is a gradient of the resistance force (3) within a migrating slug, being high in the prestalk region and much lower in the prespore region (Inouye and Takeuchi, 1979), cells will normally sort themselves out in the slug by the magnitude of the motive force (1), and this has been proposed to be the reason as to why prestalk cells are positioned in the anterior region of a slug. By the same token, the sorting pattern seen in chimeric slugs would result if the motive force of mutant prestalk cells is smaller than that of wild-type prestalk cells but still stronger than that of wild-type prespore cells, which in turn is large compared to the motive force of mutant prespore cells. The rearward sorting of mutant prespore cells within the prespore zone of mixed slugs indicates that talin B has an effect within prespore cells as well.

In 1:1 mixtures of wild-type and mutant cells, this sorting pattern persisted throughout slug migration and culmination, indicating that talin B continues to function throughout morphogenesis. The failure of morphogenesis in cell aggregates containing large fractions of mutant cells indicates that the defect of mutant cells in locomotion becomes even worse

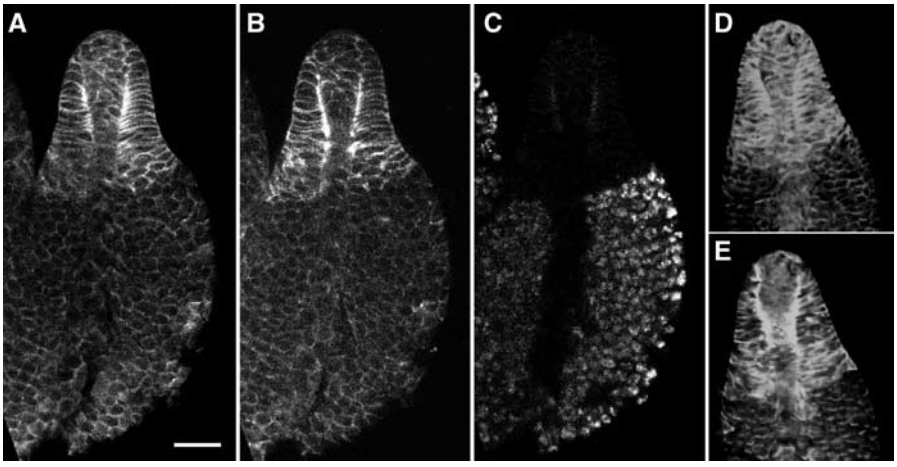

Figure 7 Distribution of talin B, F-actin and myosin II in developing fruiting bodies. (**A–C**) Confocal section showing talin B antibody (A), phalloidin (B) and PSV antibody (C) staining of a developing fruiting body of Ax2. (**D, E**) Confocal section of a developing fruiting body of GFP-myosin-expressing strain showing talin B antibody staining (D) and GFP fluorescence (E). All pictures are with the same magnification. Scale bar: 20 μm.

if there are not enough wild-type cells around, and further suggests that even wild-type cells become unable to move efficiently if totally surrounded by mutant cells. This can be explained if talin B is also required for a cell to be an effective substratum for locomotion of other cells.

Function of talin B

Double staining with fluorescent phalloidin indicated colocalisation of talin B with actin filaments in the cell cortex at cell adhesion sites, which, together with the presence of two highly conserved F-actin-binding domains in the talin B molecule (Tsujioka *et al*, 1999), suggests that talin B interacts with F-actin in the membrane regions at the sites of cell–cell and cell–substrate adhesion. Although cell adhesion molecules that interact with talin have not been identified in *Dictyostelium*, it is reasonable to expect that there might exist adhesion molecules with functions similar to metazoan β-integrins. With this assumption, the lack of talin B in a cell would result in the failure of force transmission from the actin-based cytoskeleton to the extracellular substratum on which the cell crawls. This would also account for the reduced effective force and defective movements of wild-type cells in chimaeras when outnumbered by *talB* mutant cells; a wild-type cell surrounded by mutant cells would have to get traction from the mutant's cell adhesion molecules, which are less firmly linked to the cytoskeleton due to the lack of talin B.

The reduced resistance in *talB* mutant cells found in the motive force measurement experiments (Figure 2A) can also be explained by the proposed role of talin B. This resistance force corresponds to the force (2) discussed in the previous section. In a cell undergoing fast and continuous movement, the cytoskeletal components must be rapidly recycled for reuse in the extending pseudopods in order to maintain the architecture of its locomotion machinery (Janson and Taylor, 1993). For this, actin filaments would need to be detached from the cell membrane at the rear of the cell, and the force required for such detachment would be proportional to the number of molecules linking them to the membrane. In fast-moving cells, which translocate by extending large pseudopodia, detachment of actin filaments from the cell membrane at the leading edge is also required for pseudopod extension (Yoshida and Inouye, 2001). It has been demonstrated in isolated *Dictyostelium* cells at the single-cell stage that talin A antagonises the detachment of the cell membrane from the cortical cytoskeleton (Merkel *et al*, 2000), and it would be expected that talin B does the same in cells at the multicellular stage.

If the speckled distribution of talin B on the cell membrane corresponds to the positions of adhesion structures of the cells, they are much smaller in size and more numerous than typical focal adhesions in animal cells. The lack of large focal adhesions would be advantageous for turnover of components of adhesion structures in such fast-moving cells as *Dictyostelium*, which can cover a distance of its own length within 30 s. The large number would be necessary to withstand large stress loaded on the membrane of individual cells within slugs. The results of our force measurements suggest that a single cell at the multicellular stage with a mean surface area of 150 μm^2 (value estimated from confocal sections of slugs) can exert a force of ca. 15 nN upon the surrounding tissues with a stress in the order of 100 Pa (i.e. pN μm^{-2}). Considering that about half the force is dependent on talin B, it can be estimated that talin B is involved in transmission of force of some 40 pN per fluorescent spot of antibody staining on average. In fibroblasts, Jiang *et al* (2003) demonstrated talin 1-dependent links between extracellular matrix and cytoskeleton that can be broken by a force of 2 pN. If a similar mechanism applies to talin B, the above figures may reflect the number of talin B molecules present in the complex, or possibly suggest the presence of reinforcement mechanisms that require this protein (Giannone *et al*, 2003).

Finally, it should be noted that talin A does not compensate for the defects of talin B even though it is expressed at a significant level during morphogenesis, whereas talin B does not rescue *talA* mutant cells, which show defects at single-cell stages (Kreitmeier *et al*, 1995; Tsujioka *et al*, 1999). Also, *talA* mutant cells are normal at the multicellular stages without showing any apparent motility defects as observed with the *talB* mutants (Niewöhner *et al*, 1997; our unpublished observations). If there is still some overlap in function between these talins, it will be small, and how this division

of work within a cell is accomplished is another interesting question to be addressed.

Materials and methods

Strains and conditions for growth and development

Dictyostelium discoideum Ax2 (referred to as wild type in this paper, which is an axenic derivative of the wild-type strain NC4), HKT102, HKT104, HM1011 (*talB* mutant strains obtained by homologous recombination) and a GFP-myosin II-expressing strain (Moores *et al*, 1996) were used in the present study. Isolation and characterisation of HKT102 and HM1011 were described previously (Tsujioka *et al*, 1999). HKT104 was obtained in a similar way using a disruption construct carrying a 1.9 kb hygromycin resistance cassette (Pang *et al*, 1999) inserted between a 0.8 kb fragment of the 5′UTR (nucleotides −815 to −20) of *talB* generated by PCR and a 2.6 kb *Kpn*I fragment of the coding region (nucleotides 780–3380). Transformed cells were selected with 50 μg ml^{-1} hygromycin (Wako). Axenic strains were grown in axenic medium (Sussman, 1987) or in association with *Escherichia coli* B/r or *Klebsiella aerogenes*. The *lacZ* reporter constructs *ecmAO-lacZ*, *ecmB-lacZ* and *cotC-lacZ* were introduced by electroporation, and transformant clones were selected and maintained in medium containing 20 μg ml^{-1} G418.

Cells were allowed to develop at 22°C on 1% water agar or on cellulose nitrate filter (Advantec) on 1% agar buffered with 20 mM Na/K_2 phosphate, pH 6.4. For whole-mount staining experiments, cells were allowed to develop on washed Millipore filter (type HV) placed on two layers of filter paper (Whatman no. 3) soaked with 20 mM potassium phosphate buffer, pH 6.0 or 7.0.

Preparation of migrating slugs for motive force measurements

Growth phase cells were collected at a cell density of ca. 5×10^6 cells ml^{-1}, washed once in phosphate buffer (pH 6.0), and the cell number was counted using a haemocytometer after appropriate dilution. Cell suspensions of Ax2 alone and 1:1 mixture were separately plated on 2% water agar plates, and incubated at 22°C in a humidified chamber. Chimeric and wild-type slugs that formed next day were subjected to motive force measurement.

Measurement of motive force

Motive force of a migrating slug was measured essentially by the method described earlier (Inouye and Takeuchi, 1980). Agar capillaries of 50–120 μm bore were made with purified agar (Difco, 4% in water) in a thin rectangular tunnel of a chamber made of acrylic resin and a slide glass. A small block of agar carrying a migrating slug was cut out from the plate and placed beside the orifice of the agar capillary in such a way that the tip of the slug pointed towards it. The chamber was placed in a small humidified box and illuminated from the side of the chamber opposite to the orifice in order to encourage the slug (by phototaxis) to proceed into the agar capillary. When the entire slug was in the capillary, with its all sides attached to the inner face of the capillary, the chamber was connected to a manometer and a rubber bulb for the control of the hydrostatic pressure, and the advancement of the anterior end of the slug under various hydrostatic pressures was recorded with a low observation light (wavelength >600 nm) at a rate of 4 s frame^{-1} with a ×20 objective using an inverted microscope (Nikon, TMD) and a video camera (Tokyo Denshi, CS8310) connected to a personal computer via an image grabber board (Scion, AG-5). Advancement of the tip over a period of >80 s was recorded for each pressure at least in duplicate. The length and width of the slug were determined right before and after the speed measurement. NIH Image (developed at the US National Institutes of Health and available at http://rsb.info.nih.gov/nih-image/) was used for the control of image capturing and data analysis.

Cell motility assay

Ax2 and *talB* mutant cells were allowed to develop separately on membrane filters to obtain homogeneous populations of tight mounds. After visually checking the morphology of the mounds with a dissection microscope, they were collected from the membrane filters into chilled 20 mM Na/K_2 phosphate buffer (pH 6.4) and disaggregated by three rounds of forced passage through a 26G or 27G needle. The motility of disaggregated cells responding to a cAMP gradient was examined under conditions with and without strong mechanical resistance. To produce the strong resistance condition, ca. 1 μl of cell suspension was placed on 1% buffered agar and overlaid with a thin sheet of 2% agar cut into ca. 8 mm × 8 mm. To produce weak resistance condition, the amount of cell suspension was increased three- to four-fold and 1% agar was used as the top agar. A fine glass capillary (Eppendorf, Sterile Femtotips) containing 1 mM cAMP (carboxyfluorescein was included for checking the gradient formation in some experiments) was stuck into the agar overlay, and movement of cells near the capillary tip was recorded on a time-lapse video cassette recorder (National, AG-6011A) or using the same system as described in the previous section. To quantify the movement towards the cAMP source, the numbers of cells that crossed the circle of radius 32 μm centred at the tip of the capillary inward and outward were scored over a period of 15 min. Cells that initially located outside the range of 68 or 100 μm, depending on the cell density, from the tip of the capillary were excluded from the scores. The mean velocity of cell locomotion was measured by tracking the cell centroid at intervals of 60 s.

Measurement of traction force

Polyacrylamide substrata were made according to Dembo and Wang (1999) with several modifications. The composition of the substrata used was 3.95–6.95% acrylamide, 1% allylamine and 0.05% bisacrylamide in potassium phosphate (pH 6.0), containing fluorescent marker beads (FluoSpheres, 0.2 μm diameter, Molecular Probes). The substratum made on a coverglass (22 mm × 40 mm) was put in a plastic dish with a rectangular hole (ca. 18 mm × 32 mm) in its bottom. Thick water agar was placed in the rest of the plate to keep humid. About 3 μl of cell suspension was placed on the substratum and, after the cells were settled, the buffer was removed as much as possible. A small sheat of polyacrylamide of the same composition without maker beads was gently overlaid. Cells showing directional movement were chosen for simultaneous fluorescence and transmission recording at 1–5 s intervals using a confocal microscope (Zeiss, LSM410) with ×40 Neofluar lens. The rigidity of the substrata was calibrated immediately after each set of recordings with a precalibrated fine glass needle made with a microelectrode puller. Since mechanical properties of the substrata (typical values of Young's modulus and Poisson's ratio being 3.6 kPa and 0.35, respectively) were subject to variations, these calibrations were used for correction of the results. The fluorescence images of the same visual fields with and without cells were processed by a high-pass filter (Zamir *et al*, 1999), and analysed using NIH Image to obtain the coordinates and displacements of marker beads. In some cases where depression of the substratum under the cell was detectable, centripetal displacements of the markers caused by volume exclusion by the cell were calculated using the Boussinesq equations (Landau and Lifshitz, 1970) from the magnitudes of the depression obtained by z-scanning, and subtracted from the actual displacements. In these calculations, the contributions of the tangential forces were estimated to be sufficiently small to be ignored relative to the vertical forces. Force vectors were obtained from the displacement data by the Tikhonov regularisation method as described by Schwarz *et al* (2002). Young's modulus and Poisson's ratio of the substrata were determined based on the methods of Dembo and Wang (1999) and Takigawa *et al* (1996), respectively.

Generation of polyclonal antibody against talin B

A region of talin B showing low sequence similarity to talin A was expressed as a histidine-tagged fusion protein in *E. coli*. For this, the 416 bp *Eco*RI–*Acc*I fragment of the gene was inserted into pUC119 that had been cut with the same enzymes. The *Eco*RI–*Hin*dIII fragment containing the insert was cut out from the plasmid and inserted into pTrcHisB (Invitrogen), which was transfected into *E. coli* strain JM109. Expression of the fusion protein was induced by addition of IPTG to a final concentration of 1 mM, and production of a fusion protein of the predicted size was confirmed by SDS–PAGE of bacterial lysates. The fusion protein was purified from the bacterial lysates using a nickel affinity column (Pharmacia, HisTrap), and used for the production of rabbit polyclonal antibody (Takara Custom Services). The specificity of the antibody was checked on Western blots of Ax2 cell lysates (see Figure 1). In Western blotting experiments, specific binding was visualised by

reaction with an alkaline phosphatase-conjugated anti-rabbit antibody followed by incubation with BCIP/NBT (Sigma). For immunohistological staining, nonspecific binding of the antibody was eliminated by absorbing the antisera with an excess of methanol-fixed HM1011 cells at the tight mound stage (10^9 cells for 3 ml of 3000-fold diluted antisera).

Histological methods

Isolated cells and tissues were fixed in ethanol containing 1% formaldehyde at −20 and 4°C, respectively, washed in PBS–Tween (10 mM phosphate buffer (pH 7.0), 0.9% NaCl, 0.05% Tween 20), and preincubated with PBS–Tween containing 0.5% each of bovine serum albumin and gelatin before staining.

For immunostaining, specimens were incubated with preabsorbed anti-talin B antiserum (1:9000 dilution) overnight or longer at 4°C, washed three times in PBS–Tween, then incubated with affinity-purified goat anti-rabbit IgG conjugated with either Alexa 488 (Molecular Probes), TRITC or Cy5 (Chemicon International) overnight at 4°C. Control staining was performed with a preimmune serum or with the omission of primary antibody, both giving almost undetectable fluorescence under the same optical conditions as used for the experimentals. F-actin and PSVs were visualised by staining with TRITC-phalloidin (Sigma) and FITC- or TRITC-conjugated anti-*D. mucoroides* spore IgG, respectively. The samples were observed with a confocal microscope (Zeiss LSM410) with a ×63 Neofluar objective (NA 1.40). For quantitative analysis of antibody staining, confocal images recorded at a magnification of 1 pixel = 56.6 nm were inverted and smoothed to reduce noise by averaging 5 × 5 pixels for each pixel. All image analyses were performed with NIH Image on a personal computer.

For *lacZ* staining, migrating slugs on filters were fixed with 0.5% glutaraldehyde and stained with X-gal (Jermyn and Williams, 1991).

Acknowledgements

We thank S Yumura and J Spudich for the GFP-myosin strain, R Kay for HM1011, D Knecht for the hygromycin-resistant plasmid, and J Williams and V Nanjundiah for comments on an earlier version of the manuscript.

References

Albigès-Rizo C, Frachet P, Block MR (1995) Down regulation of talin alters cell adhesion and the processing of the α5β1 integrin. *J Cell Sci* **108:** 3317–3329

Bolton SJ, Barry ST, Mosley H, Patel B, Jockusch BM, Wilkinson JM, Critchley DR (1997) Monoclonal antibodies recognizing the N- and C-terminal regions of talin disrupt actin stress fibers when microinjected into human fibroblasts. *Cell Motil Cytoskeleton* **36:** 363–376

Brown NH, Gregory SL, Rickoll WL, Fessler LI, Prout M, White RA, Fristrom JW (2002) Talin is essential for integrin function in *Drosophila*. *Dev Cell* **3:** 569–579

Burridge K, Connell L (1983) A new protein of adhesion plaques and ruffling membranes. *J Cell Biol* **97:** 359–367

Chen PX, Ostrow BD, Tafuri SR, Chisholm RL (1994) Targeted disruption of the *Dictyostelium* RMLC gene produces cells defective in cytokinesis and development. *J Cell Biol* **127:** 1933–1944

Coates JC, Harwood AJ (2001) Cell–cell adhesion and signal transduction during *Dictyostelium* development. *J Cell Sci* **114:** 4349–4358

Cole SL (1997) The isolation and characterisation of two genes required for tip formation in *Dictyostelium discoideum*. DPhil Thesis, University College London

Critchley DR (2000) Focal adhesions—the cytoskeletal connection. *Curr Opin Cell Biol* **12:** 133–139

Dembo M, Wang Y-L (1999) Stress at the cell-to-substrate interface during locomotion of fibroblasts. *Biophys J* **76:** 2307–2316

Early A, Abe T, Williams J (1995) Evidence for positional differentiation of prestalk cells and for a morphogenetic gradient in *Dictyostelium*. *Cell* **83:** 91–99

Freeze H, Loomis W (1977) The isolation and characterization of a component of the surface sheath of *Dictyostelium discoideum*. *J Biol Chem* **252:** 820–824

Giannone G, Jiang G, Sutton DH, Critchley DR, Sheetz MP (2003) Talin1 is critical for force-dependent reinforcement of initial integrin–cytoskeleton bonds but not tyrosine kinase activation. *J Cell Biol* **163:** 409–419

Grimson MJ, Coates JC, Reynolds JP, Shipman M, Blanton RL, Harwood AJ (2000) Adherens junctions and β-catenin-mediated cell signalling in a non-metazoan organism. *Nature* **408:** 727–731

Haberstroh L, Firtel RA (1990) A spatial gradient of expression of a cAMP-regulated prespore cell type-specific gene in *Dictyostelium*. *Genes Dev* **4:** 596–612

Inouye K (2003) Pattern formation by cell movement in closely-packed tissues. In *Morphogenesis and Pattern Formation in Biological Systems*, Sekimura T, Noji S, Ueno N, Maini PK (eds) pp 191–202. Tokyo: Springer-Verlag

Inouye K, Takeuchi I (1979) Analytical studies on migrating, movement of the pseudoplasmodium of *Dictyostelium discoideum*. *Protoplasma* **99:** 289–304

Inouye K, Takeuchi I (1980) Motive force of the migrating pseudoplasmodium of the cellular slime mould *Dictyostelium discoideum*. *J Cell Sci* **41:** 53–64

Janson LW, Taylor DL (1993) *In vitro* models of tail contraction and cytoplasmic streaming in amoeboid cells. *J Cell Biol* **123:** 345–356

Jiang G, Giannone G, Critchley DR, Fukumoto E, Sheetz MP (2003) Two-piconewton slip bond between fibronectin and the cytoskeleton depends on talin. *Nature* **424:** 334–337

Jermyn KA, Williams JG (1991) An analysis of culmination in *Dictyostelium* using prestalk and stalk-specific cell autonomous markers. *Development* **111:** 779–787

Kreitmeier M, Gerisch G, Heizer C, Müller-Taubenberger A (1995) A talin homologue of *Dictyostelium* rapidly assembles at the leading edge of cells in response to chemoattractant. *J Cell Biol* **129:** 179–188

Landau LD, Lifshitz EM (1970) *Theory of Elasticity. Course of Theoretical Physics*, 2nd edn, Vol. 7 Oxford: Pergamon Press

McCann RO, Craig SW (1997) The I/LWEQ module: a conserved sequence that signifies F-actin binding in functionally diverse proteins from yeast to mammals. *Proc Natl Acad Sci USA* **94:** 5679–5684

Merkel R, Simson R, Simson DA, Hohenadl M, Boulbitch A, Wallraff E, Sackmann E (2000) A micromechanic study of cell polarity and plasma membrane cell body coupling in *Dictyostelium*. *Biophys J* **79:** 707–719

Monkley SJ, Zhou XH, Kinston SJ, Giblett SM, Hemmings L, Priddle H, Brown JE, Pritchard CA, Critchley DR, Fassler R (2000) Disruption of the talin gene arrests mouse development at the gastrulation stage. *Dev Dyn* **219:** 560–574

Moores SL, Sabry JH, Spudich JA (1996) Myosin dynamics in live *Dictyostelium* cells. *Proc Natl Acad Sci USA* **93:** 443–446

Niewöhner J, Weber I, Maniak M, Müller-Taubenberger A, Gerisch G (1997) Talin-null cells of *Dictyostelium* are strongly defective in adhesion to particle and substrate surfaces and slightly impaired in cytokinesis. *J Cell Biol* **138:** 349–361

Nuckolls GH, Romer LH, Burridge K (1992) Microinjection of antibodies against talin inhibits the spreading and migration of fibroblasts. *J Cell Sci* **102:** 753–762

Pang KM, Lynes MA, Knecht DA (1999) Variables controlling the expression level of exogenous genes in *Dictyostelium*. *Plasmid* **41:** 187–197

Priddle H, Hemmings L, Monkley S, Woods A, Patel B, Sutton D, Dunn GA, Zicha D, Critchley DR (1998) Disruption of the talin gene compromises focal adhesion assembly in undifferentiated but not differentiated embryonic stem cells. *J Cell Biol* **142:** 1121–1133

Raper KB (1940) Pseudoplasmodium formation and organization in *Dictyostelium discoideum*. *J Elisha Mitchell Sci Soc* **56:** 241–282

Rubin J, Robertson A (1975) The tip of the *Dictyostelium discoideum* pseudoplasmodium as an organizer. *J Embryol Exp Morphol* **33:** 227–241

Schwarz US, Balaban NQ, Riveline D, Bershadsky A, Geiger B, Safran SA (2002) Calculation of forces at focal adhesions from elastic substrate data: the effect of localized force and the need for regularization. *Biophys J* **83:** 1380–1394

Simson R, Wallraff E, Faix J, Niewöhner J, Gerisch G, Sackmann E (1998) Membrane bending modulus and adhesion energy of wild-type and mutant cells of *Dictyostelium* lacking talin or cortexillins. *Biophys J* **74:** 514–522

Springer ML, Patterson B, Spudich JA (1994) Stage-specific requirement for myosin II during *Dictyostelium* development. *Development* **120:** 2651–2660

Sternfeld J, David CN (1981) Cell sorting during pattern formation in *Dictyostelium*. *Differentiation* **20:** 10–21

Sussman M (1987) Cultivation and synchronous morphogenesis of *Dictyostelium* under controlled experimental conditions. In *Methods in Cell Biology,* Spudich JA (ed) Vol. 28 , pp 9–29. Orlando, FL: Academic Press

Takigawa T, Morino Y, Urayama K, Masuda T (1996) Poisson's ratio of polyacrylamide (PAAm) gels. *Polym Gels Networks* **4:** 1–5

Tidball JG, O'Halloran T, Burridge K (1986) Talin at myotendinous junctions. *J Cell Biol* **103:** 1465–1472

Traynor D, Tasaka M, Takeuchi I, Williams J (1994) Aberrant pattern formation in myosin heavy chain mutants of *Dictyostelium*. *Development* **120:** 591–601

Tsujioka M, Machesky LM, Cole SL, Yahata K, Inouye K (1999) A unique talin homologue with a villin headpiece-like domain is required for multicellular morphogenesis in *Dictyostelium*. *Curr Biol* **9:** 389–392

Umeda T, Inouye K (2004) Cell sorting by differential cell motility: a model for pattern formation in *Dictyostelium*. *J Theor Biol* **226:** 215–224

Williams JG, Jermyn KA, Duffy KT (1989) Formation and anatomy of the prestalk zone of *Dictyostelium*. *Development* **107** (Suppl)**:** 91–98

Witke W, Schleicher M, Noegel AA (1992) Redundancy in the microfilament system—abnormal development of *Dictyostelium* cells lacking two F-actin cross-linking proteins. *Cell* **68:** 53–62

Yoshida K, Inouye K (2001) Myosin II-dependent cylindrical protrusions induced by quinine in *Dictyostelium*: antagonizing effects of actin polymerization at the leading edge. *J Cell Sci* **114:** 2155–2165

Zamir E, Katz B-Z, Aota S, Yamada KM, Geiger B, Kam Z (1999) Molecular diversity of cell–matrix adhesions. *J Cell Sci* **112:** 1655–1669